Magnetic microstructure of a textured Nd-Fe-B sintered magnet characterized by small-angle neutron scattering

E.A. Périgo[1], D. Mettus[1], E.P. Gilbert[2], P. Hautle[3], N. Niketic[3], B. van den Brandt[3], J. Kohlbrecher[3], P. McGuiness[4], Z. Fu,[5] and A. Michels[1]

[1] Physics and Materials Science Research Unit, University of Luxembourg, 162a avenue de la Faïencerie, L-1511 Luxembourg, Grand Duchy of Luxembourg

[2] Bragg Institute, ANSTO, Locked Bag 2001, Kirrawee DC, NSW 2232, Australia

[3] Paul Scherrer Institute, CH-5232 Villigen PSI, Switzerland

[4] Institute of Metals and Technology, Lepi pot 11, Sl-1000 Ljubljana, Slovenia

[5] Jülich Centre for Neutron Science (JCNS), Forschungszentrum Jülich GmbH, Outstation at MLZ, Lichtenbergstraße 1, D-85747 Garching, Germany

ABSTRACT

We report the results of a small-angle neutron scattering (SANS) study on the magnetic microstructure of a textured Nd-Fe-B-based sintered permanent magnet. By combining unpolarized and polarized SANS (SANSPOL), we demonstrate that a number of important conclusions regarding the microscopic spin structure can be made. Specifically, the applied-field dependence of the unpolarized neutron data is in agreement with the existence of long-range spin-misalignment fluctuations, i.e., deviations of the magnetization from the mean direction on a real-space length-scale up to the micron range. In addition, measurements with polarized neutrons provide evidence for the presence of coupled nanometer-scale fluctuations in the nuclear and longitudinal magnetic scattering-length density.

***Keywords*:** Nd-Fe-B, polarized neutron scattering, small-angle neutron scattering, coercive field

Corresponding author: Dr. Elio Alberto Périgo
Address: 162a, Avenue de la Faiencerie – Luxembourg – L1511 – Luxembourg
Phone: 352 46 66 44 6992 – Fax : 352 46 66 44 6330 – email : eaperigo@ieee.org

I. Introduction

Nd-Fe-B-based sintered magnets have been continuously investigated for the last three decades due to their technological relevance as materials used in energy-related applications (e.g., motors and wind turbines) [1]. A crucial issue in research on Nd-Fe-B-based magnets is the understanding of the magnetization-reversal process, which eventually may result in the preparation of dysprosium and terbium-free Nd-Fe-B alloys with characteristic magnetic properties (coercivity, remanence, maximum energy product) that guarantee their performance also at the operating temperatures of motors (up to ~ 200 °C) [2].

In order to achieve this goal, the combination of advanced characterization techniques such as aberration-corrected high-resolution transmission electron microscopy and three-dimensional atom-probe tomography (e.g., [3,4]) with *ab initio* calculations and numerical micromagnetic modeling [5] is required. Indeed, recent studies have provided important information regarding the nature (chemical composition, crystalline structure, ferro- or paramagnetic) of the intergranular Nd-rich phases in Nd-Fe-B sintered magnets, which decisively determine the coercivity mechanism of these materials [5].

Magnetic neutron scattering, in particular, small-angle neutron scattering (SANS) is another important technique for characterizing the bulk magnetic microstructure of engineering permanent magnetic materials (see Ref. [6] for a recent review). Conventional magnetic SANS provides information on variations of both the magnitude and orientation of the magnetization on a nanometer length scale (~ 1-300 nm). However, this method has only recently been employed for studying the spin microstructure of this class of materials: for instance, the size and field dependence of inhomogeneously magnetized regions (during magnetization reversal) in Nd-Fe-B-based nanocomposites [7] and in isotropic sintered Nd-Fe-B [8] were determined; quantitative analysis of field-dependent SANS data in terms of micromagnetic theory allows one to estimate the value of the exchange-stiffness constant A [9,10], and the observation of the so-called spike anisotropy in the magnetic SANS cross section [9] has been explained with the formation of flux-closure patterns (pole-avoidance principle). Moreover, nanocrystalline textured Nd-Fe-B magnets prepared by hot deformation have also been investigated using SANS, specifically, the effects of grain-boundary

diffusion on the magnetization-reversal process have been studied [11,12,13]. The authors of Refs. [11,12,13] report that in magnetically isolated (infiltrated) samples, the spatial fluctuation of magnetic moments appears to be reduced as compared to the as-deformed samples.

In this work, we study the magnetic microstructure of an anisotropic (textured) Nd-Fe-B-based sintered magnet using magnetic SANS. We will demonstrate that the combined use of unpolarized and spin-polarized neutrons provides powerful means for the study of engineering magnetic materials.

II. Experimental

Commercially available Nd-Fe-B-based N38 *textured* sintered magnets have been used in this study. The magnetic characterization has been carried out at room temperature on a needle-shaped sample ($7 \times 1 \times 1$ mm^3) using a vibrating sample magnetometer ($\mu_0 H_{max} = 14$ T). The microstructure has been characterized by scanning electron microscopy (SEM) and phase identification has been performed by X-ray diffraction (Cu-Kα radiation, Bragg-Brentano geometry). The texture degree, given by the $\langle \cos \Theta \rangle$ parameter, has been calculated by applying the procedure reported in Ref. [14].

The SANS experiments have been performed at $T = 295$ K at the instrument Quokka (ANSTO, Australia [15]) using *unpolarized* neutrons with a mean wavelength of $\lambda = 4.8$ Å ($\Delta\lambda/\lambda \cong 10$ % (FWHM)). The external magnetic field $\mathbf{H}_0$ (provided by a cryomagnet) was applied perpendicular to the wave vector $\mathbf{k}_0$ of the incoming neutron beam and parallel to the easy (texture) axis of the specimen (see Fig. 1). Neutron data were corrected for background scattering (empty sample holder), transmission and detector efficiency, and set to absolute units using a calibrated attenuated direct-beam measurement. Additional neutron experiments have also been performed at the instruments KWS-3 (JCNS, Germany) and SANS-I (PSI, Switzerland) with *unpolarized* and *spin-polarized* neutrons [16], respectively. For further details regarding polarized SANS, we refer the reader to Refs. [17,18].

III. SANS cross sections

In this section, we will briefly recall the basic equations (as required in this work) of magnetic

SANS using unpolarized and spin-polarized neutrons [6]. When the applied magnetic field $\mathbf{H}_0 \,||\, \mathbf{e}_z$ is perpendicular to the wave vector $\mathbf{k}_0$ of the incoming neutron beam (Fig. 1), the elastic nuclear and magnetic SANS cross section at momentum-transfer vector $\mathbf{q} \cong (0, q_y, q_z) = q\ (0, \sin\theta, \cos\theta)$ can be expressed as:

$$\frac{d\Sigma}{d\Omega}(\mathbf{q}) = \frac{8\pi^3}{V} b_H^2 \left[\frac{|\tilde{N}|^2}{b_H^2} + \left|\tilde{M}_x^2\right| + \left|\tilde{M}_y^2\right| \cos^2\theta + \left|\tilde{M}_z^2\right| \sin^2\theta - \left(\tilde{M}_y \tilde{M}_z^* + \tilde{M}_y^* \tilde{M}_z\right) \sin\theta \cos\theta\right], \quad (1)$$

where V is the scattering volume, $b_H = 2.91 \times 10^8$ $A^{-1}m^{-1}$, $\tilde{N}(\mathbf{q})$ refers to the nuclear scattering amplitude, $\tilde{M}_{x,y,z}(\mathbf{q})$ represent the Fourier components (in Cartesian coordinates) of the magnetization vector field $M_{x,y,z}(\mathbf{r})$, the symbol "*" indicates the complex-conjugated quantity, and $\theta = \angle(\mathbf{q}, \mathbf{H}_0)$.

For a polarized incident beam and no polarization analysis of the scattered beam, the two so-called SANSPOL spin-up and spin-down (relative to the guide field) cross sections $d\Sigma^+/d\Omega$ and $d\Sigma^-/d\Omega$ read [6]:

$$\frac{d\Sigma^{\pm}}{d\Omega}(\mathbf{q}) = \frac{8\pi^3}{V} b_H^2 \left[\begin{array}{c} \frac{|\tilde{N}|^2}{b_H^2} + \left|\tilde{M}_x^2\right| + \left|\tilde{M}_y^2\right| \cos^2\theta + \left|\tilde{M}_z^2\right| \sin^2\theta - \left(\tilde{M}_y \tilde{M}_z^* + \tilde{M}_y^* \tilde{M}_z\right) \sin\theta \cos\theta \\ \mp b_H^{-1} P \left|1 - 2f^{\pm}\right| \left(\tilde{N}\tilde{M}_z^* + \tilde{N}^*\tilde{M}_z\right) \sin^2\theta \ \pm b_H^{-1} P \left|1 - 2f^{\pm}\right| \left(\tilde{N}\tilde{M}_y^* + \tilde{N}^*\tilde{M}_y\right) \sin\theta \cos\theta \end{array}\right], \quad (2)$$

where P denotes the incident-beam polarization and f is the efficiency of the spin flipper ($f^+ = 0$ for flipper off and $f^- \cong 1$ for flipper on). The difference between both spin states yields the nuclear-magnetic interference terms, also investigated in this work, given by:

$$\frac{d\Sigma^-}{d\Omega} - \frac{d\Sigma^+}{d\Omega} = \frac{8\pi^3}{V} 2 b_H P \left|1 - 2f^{\pm}\right| \left[\left(\tilde{N}\tilde{M}_z^* + \tilde{N}^*\tilde{M}_z\right) \sin^2\theta - \left(\tilde{N}\tilde{M}_y^* + \tilde{N}^*\tilde{M}_y\right) \sin\theta \cos\theta\right] \quad (3)$$

IV. Results and discussion

The room-temperature hysteresis curves (with the texture axis parallel and perpendicular to the applied field) of the Nd-Fe-B sintered magnet is depicted in Fig. 2; it indicates an anisotropic microstructure with a coercive field (for the texture axis // $\mathbf{H}_0$) of $\mu_0 H_c$ = 1.20 T (typical for Dy-free magnets) and a remanence J_r which is ~ 8 % smaller than the polarization reached at 14 T. The XRD pattern of the magnetic specimen (data not shown) displays only some of the 2:14:1 phase peaks due to the crystallographic orientation of the sample; the degree of texture is $\langle \cos \Theta \rangle$ = 0.94. Besides, additional Bragg peaks appear which can be related to the Nd-rich phase of hexagonal structure (located mainly at triple points and with less than 3 % wt. in total). Both phases can be observed in the SEM micrograph shown in Fig. 3.

The 2D unpolarized SANS intensity distribution of the textured Nd-Fe-B sintered magnet at 10T is displayed in Fig. 4(a); the texture axis is parallel to $\mathbf{H}_0$ (which is horizontal in the plane). Instead of the usual $\sin^2\theta$ anisotropy, which is characteristic for (nearly) saturated magnetic microstructures, the 2D intensity distribution reveals a "diamond-shaped" angular anisotropy. A similar feature has also been reported by Kreyssig *et al.* [19] on a $Nd_2Fe_{14}B$ single crystal with the *c*-axis oriented parallel to the incident neutron beam; at zero applied magnetic field, the origin of this particular pattern has been explained in [19] in terms of a fractal domain structure. However, our data do not support such a conclusion, since at an applied field of 10 T the Nd-Fe-B specimen is in the approach-to-saturation regime (compare Fig. 2), which suggests the absence of a domain structure.

The azimuthally-averaged neutron data (Fig. 4(b)) clearly show that within the studied *q*-range the unpolarized SANS cross section is effectively field-independent between +10 T and -1.2 T = $\mu_0 H_c$; in other words, the scattering-length density contrast which is responsible for the observed $d\Sigma/d\Omega$ is constant for 0.04 $nm^{-1} < q < 2.0$ nm^{-1}. Since magnetic scattering due to misaligned spins is usually strongly field-dependent (compare Eq. (1) and e.g. Fig. 3 in [6]), this observation suggests a very weak spin-misalignment scattering contribution to $d\Sigma/d\Omega$. Moreover, the field-independence of $d\Sigma/d\Omega$ in Fig. 4(b) is indicative of an appreciable nuclear SANS signal in the textured Nd-Fe-B magnet. It is also worth noting the broad shoulder in $d\Sigma/d\Omega$ at $q \cong 0.5$ nm^{-1} (dashed square in Fig. 4(b)), which, in

real-space, corresponds to structure sizes of the order of ~ 1-10 nm. Possible features in the microstructure which could give rise to the hump are nanometer-sized precipitates within the Nd-rich phases (at triple points or grain boundaries) [20,21].

Magnetic-field-dependent measurements on the very small-angle neutron scattering (VSANS) diffractometer KWS-3 (JCNS, Germany) allow us to access the magnetization Fourier components at small momentum transfers (see Fig. 4(c)). The data provide clear evidence that spin-misalignment fluctuations in textured Nd-Fe-B are existing on a length scale up to the micron range. Between +2.2 T and the remanent state, the total cross section changes by a factor of about two (for $q < 0.01$ nm^{-1}), which clearly points towards magnetic scattering due to large-sized inhomogeneously magnetized regions within the sample (related, e.g., to microstructural defects such as grain boundaries) [6]. At the smallest q-values, the data in Fig. 4(c) suggest a trend to "saturate" (no field dependence), which implies the absence of a change in the scattering contrast.

Polarized neutrons are very useful in the study of magnetic materials, for instance, for separating weak magnetic signals from strong nuclear scattering [22] (see above). Experiments with a polarized incident neutron beam allow us to measure scattering terms that depend *linearly* on the nuclear and magnetic scattering amplitudes, instead of the usual *quadratic* dependence of the total unpolarized $d\Sigma/d\Omega$ on these terms (compare Eq. (1)). In fact, the difference between spin-up and spin-down measurements, given by Eq. (3), depends on interference terms $\tilde{N}\tilde{M}_z$ and $\tilde{N}\tilde{M}_y$. Figure 5 displays $\frac{d\Sigma^-}{d\Omega} - \frac{d\Sigma^+}{d\Omega}$ at $\mu_0 H_0 = 0.6$ T for the cases where the texture axis is parallel (Fig. 5(a)) and perpendicular (Fig. 5(b)) to the applied field $\mathbf{H}_0$. The anisotropy of the pattern is in *both* cases clearly of the $\sin^2\theta$ type with an elongation *perpendicular* to $\mathbf{H}_0$. From the observation that the SANSPOL data in Fig. 5(a) and 5(b) exhibit a dominant and almost "pure" $\sin^2\theta$ anisotropy, one may conclude that both Fourier components $\tilde{N}$ and $\tilde{M}_z$ are isotropic, i.e., they do not depend on the orientation θ of the scattering vector $\mathbf{q}$, only on its magnitude q. Furthermore, the dominating $\sin^2\theta$ type anisotropy (in Figs. 5(a) and 5(b)) suggests the absence of scattering terms $\tilde{N}\tilde{M}_y$ in Eq. (3), which would yield extrema roughly along the diagonals of the detector [6]. The 1D (azimuthally-averaged) data of both

difference SANSPOL cross sections (for the texture axis parallel and perpendicular to $\mathbf{H}_0$) are compared in Fig. 5(c) and no significant difference between them is noticed. Note also that Eq. (3) predicts coupled nanometer-scale fluctuations in the nuclear and longitudinal magnetic scattering-length density; for the validity of Eq. (3), it is not required that the sample is in the saturated state. In fact, by comparison to Fig. 2, it is readily inferred that at a field of 0.6 T the sample is rather subdivided into domains, but with a resulting net magnetization. SANS measurements at smaller fields result in the depolarization of the neutron beam.

V. Conclusions

We have reported the results of a small-angle neutron scattering (SANS) study of the magnetic microstructure of a textured Nd-Fe-B sintered magnet. For 0.04 $nm^{-1} < q < 2.0$ nm^{-1}, the unpolarized neutron data reveal a field-independent SANS cross section (between +10 T and $\mu_0 H_c$ = -1.2 T), which suggests a weak spin-misalignment scattering contribution in this q-range. However, our results using the technique of very small-angle neutron scattering (VSANS) disclose the existence of long-range spin-misalignment fluctuations at small momentum transfers, usually not accessible with conventional SANS. With the aid of a polarized incident neutron beam (SANSPOL), the nuclear-magnetic interference terms in the cross section could be accessed. The SANSPOL data reveal the absence of scattering terms $\tilde{N}\tilde{M}_y \sin\theta\cos\phi$ and the presence of a strong $\tilde{N}\tilde{M}_z \sin^2\theta$ anisotropy for the cases in which the texture axis is both parallel and perpendicular to the applied field $\mathbf{H}_0$. The present study demonstrates the power of the SANS technique for characterizing the magnetic microstructure of textured Nd-Fe-B magnets on a mesoscopic length scale (~ 1-1000 nm).

Acknowledgments

The authors acknowledge financial support from the National Research Fund of Luxembourg (Project No. INTER/DFG/12/07) and from the University of Luxembourg (INTERFACE 2012 project). The authors are also indebted to P. Imperia, N. Booth and G. Davidson for sample-environment support and to F. Franceschini and N. Xiong for IT support. We thank Jörg Schmauch

(Universität des Saarlandes) for the electron-microscopy work. This research is based on experiments performed at the Swiss spallation neutron source SINQ, Paul Scherrer Institute, Villigen, Switzerland.

References

[1] O. Gutfleisch, M.A. Willard, E. Brück, C.H. Chen, S.G. Sankar, J. Ping Liu, Adv. Mater. v. 23 (7) (2010), pp. 821-842,.

[2] K. Hono, H. Sepehri-Amin, Scripta Mater. v. 67 (6) (2012), pp. 530-535.

[3] Q. Liu, F. Xu, J. Wang, X. Dong, L. Zhang, J. Yang, Scripta Mater., v. 68 (9) (2013), pp. 687-690.

[4] T.T. Sasaki, T. Ohkubo, Y. Une, H. Kubo, M. Sagawa, K. Hono, Acta Mater. v. 84 (2015), pp. 506-514.

[5] T.G. Woodcock, Y. Zhang, G. Hrkac, G. Ciuta, N.M. Dempsey, T. Schrefl, O. Gutfleisch, D. Givord, Scripta Mater. v. 67 (2012), pp. 536-541.

[6] A. Michels, J. Phys.: Condens. Matter, v. 26 (2014), art. 383201.

[7] J.-P. Bick, D. Honecker, F. Döbrich, K. Suzuki, E.P. Gilbert, H. Frielinghaus, J. Kohlbrecher, J. Gavilano, E.M. Forgan, R. Schweins, P. Linder, R. Birringer, A. Michels, App. Phys. Lett., v. 102 (2013), art. 022415.

[8] E.A. Périgo, E.P. Gilbert, A. Michels, Acta Mater. v. 87 (2015), pp. 142-149.

[9] E.A. Périgo, E.P. Gilbert, K.L. Metlov, A. Michels, New. J. Phys., v. 16 (2014), art. 123031.

[10] J.-P. Bick, K. Suzuki, E.P. Gilbert, E.M. Forgan, R. Schweins, P. Lindner, C. Kübel, and A. Michels, App. Phis. Lett. v. 103 (2013), art. 122402.

[11] T. Ueno, K. Saito, M. Yano, M. Harada, T. Shoji, N. Sakuma, A. Manabe, A. Kaito, U. Keiderling, K. Ono, IEEE Trans. Magn., v. 50 (11) (2014), art 2103104.

[12] M. Yano, K. Ono, M. Harada, A. Manabe, T. Shoji, A. Kato, J. Kohlbrecher, J. Appl. Phys., v. 115 (2014), art. 17A730.

[13] K. Saito, T. Ueno, M. Yano, M. Harada, T. Shoji, N. Sakuma, A. Manabe, A. Kato, U. Keiderling, and K. Ono, J. Appl. Phys. 117 (2015), 17B302.

[14] E.A. Périgo, H. Takiishi, C.C. Motta, R.N. Faria, and N.B. Lima, J. Magn. Magn. Mater., v. 320 (2008), pp. e40-e42.

[15] E.P. Gilbert, J.C. Schultz, T.J. Noakes, Physica B, v. 385-386 (2006), pp. 1180-1182.

[16] J. Kohlbrecher and W. Wagner, J. Appl. Crystallogr. v. 33 (2000), pp. 804-806; N. Niketic, B. van den Brandt, W.Th. Wenckebach, J. Kohlbrecher, and P. Hautle, J. Appl. Crystallogr. v. 48, (2015), pp. 1514-1521.

[17] D. Honecker, A. Ferdinand, F. Döbrich, C.D. Dewhurst, A. Wiedenmann, C. Gómez-Polo, K. Suzuki, and A. Michels, Eur. Phys. J. B 76 (2010), pp. 209-213.

[18] A. Michels, D. Honecker, F. Döbrich, C.D. Dewhurst, K. Suzuki, and A. Heinemann, Phys. Rev. B 85 (2012), art. 184417.

[19] A. Kreyssig, R. Prozorov, C.D. Dewhurst, P. C. Canfield, R. W McCallum, A.I. Goldman, Phys. Rev. Lett. v. 102 (2009), art. 047204.

[20] N. Watanabe, H. Umemoto, M. Itakura, M. Nishira, K. Machida, IOP Conf. Ser.: Mater. Sci. Eng. v. 1 (2009), art. 012033.

[21] M. Yan, X. Cui, L. Yu, T. Ma, J. Mater. Sci. Technol. v. 25 (5) (2009), pp. 629-632.

[22] T. Keller, T. Krist, A. Danzig, U. Keiderling, F. Mezei, and A. Wiedenmann, Nuclear Instruments and Methods in Physics Research A, v. 451 (2000), pp. 474-479.

List of Captions

Figure 1 – Sketch of the scattering geometry.

Figure 2 – Room-temperature magnetization curve (texture axis parallel and perpendicular to the applied field) of a textured Nd-Fe-B-based sintered magnet. The magnetic properties for the texture axis // $\mathbf{H_0}$ are indicated in the inset.

Figure 3 – SEM image of the textured Nd-Fe-B magnet.

Figure 4 – (a) Total (nuclear and magnetic) unpolarized SANS cross section $d\Sigma/d\Omega$ of the textured Nd-Fe-B sintered magnet at $\mu_0 H_0$ = 10 T (logarithmic color scale). (b) Azimuthally-averaged $d\Sigma/d\Omega$ as a function of the scattering vector q at selected applied magnetic fields (see inset) (log-log scale). (c) Very small-angle neutron scattering (VSANS) data taken at KWS-3 (log-log scale). The arrow indicates the direction of increasing field.

Figure 5 – Difference between spin-up and spin-down SANS cross sections, $\frac{d\Sigma^-}{d\Omega} - \frac{d\Sigma^+}{d\Omega}$, of the textured Nd-Fe-B sintered magnet at $\mu_0 H_0$ = 0.6 T (logarithmic color scale). The texture axis is (a) parallel and (b) perpendicular to the external magnetic field (horizontal in the plane of the image). (c) Corresponding azimuthally-averaged SANSPOL cross sections (log-log scale) (solid line: $\propto q^{-4}$).

Figure 1

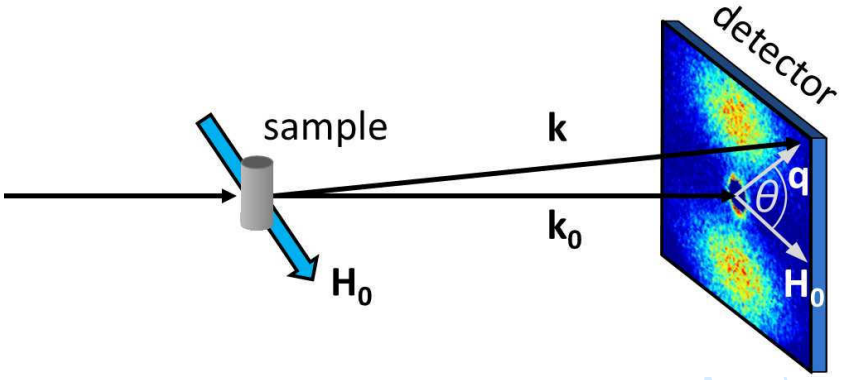

Figure 2

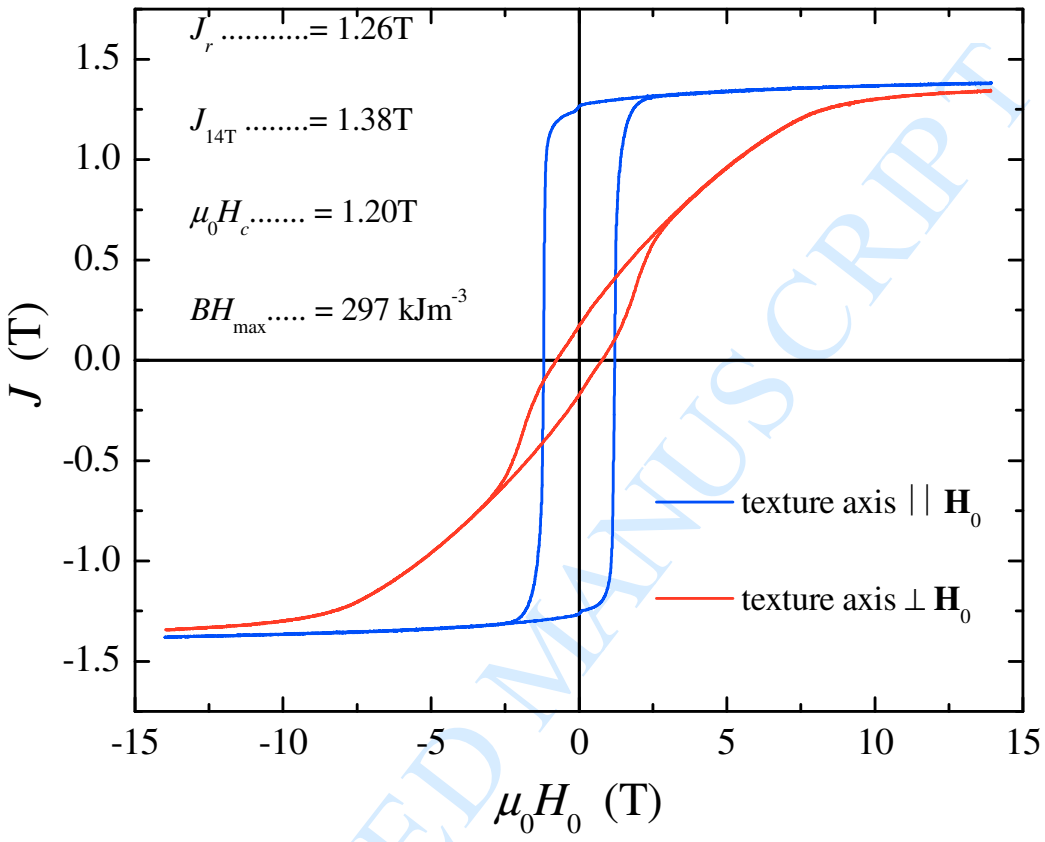

Figure 3

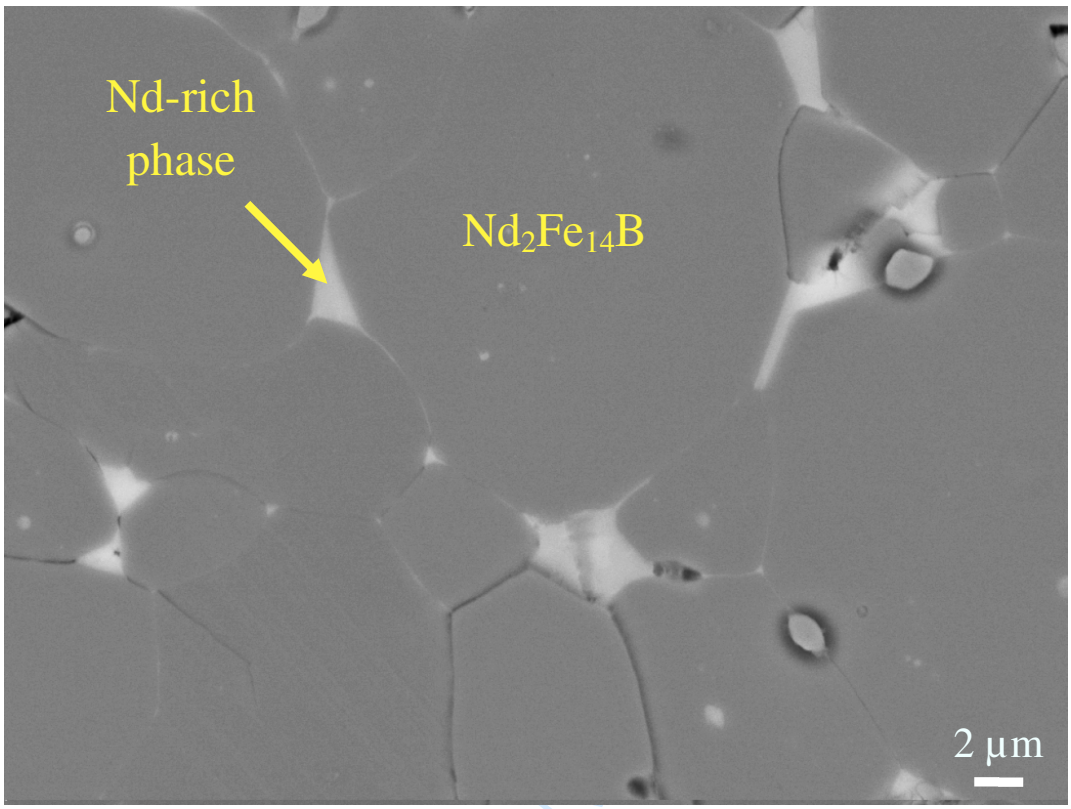

Figure 4(a)

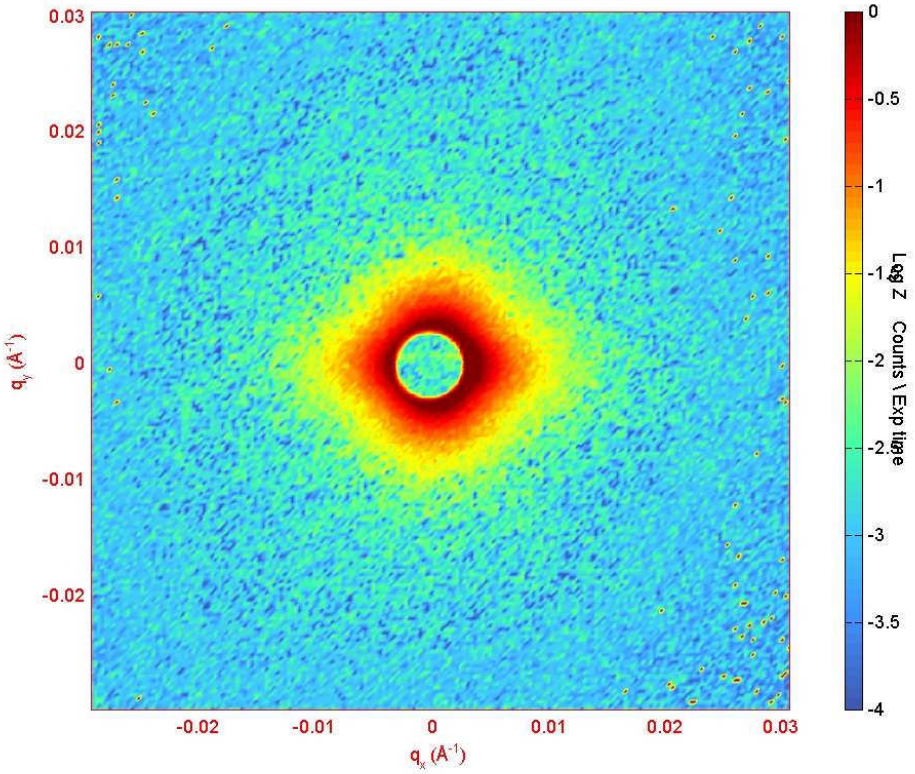

Figure 4(b)

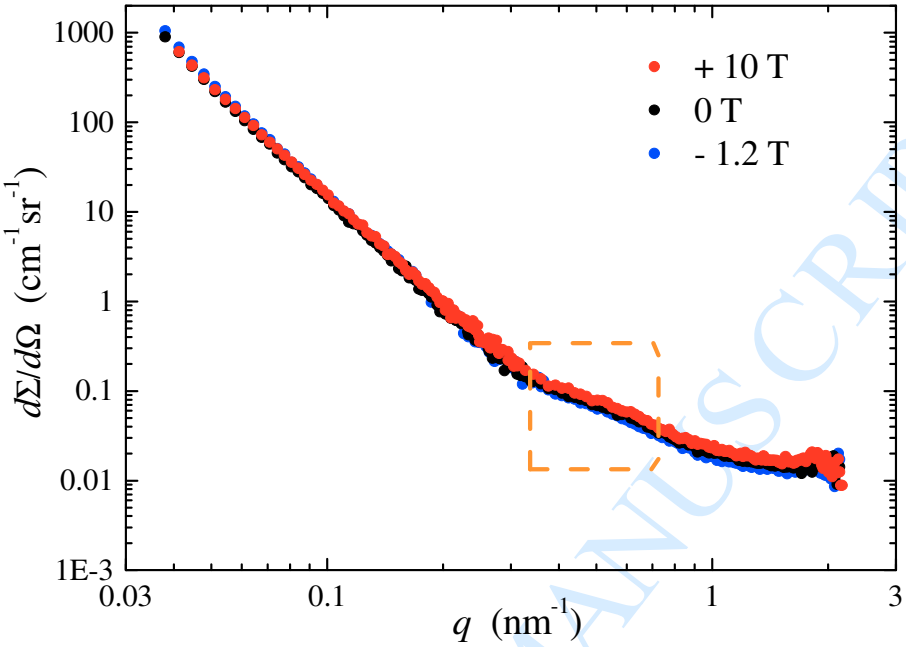

Figure 4(c)

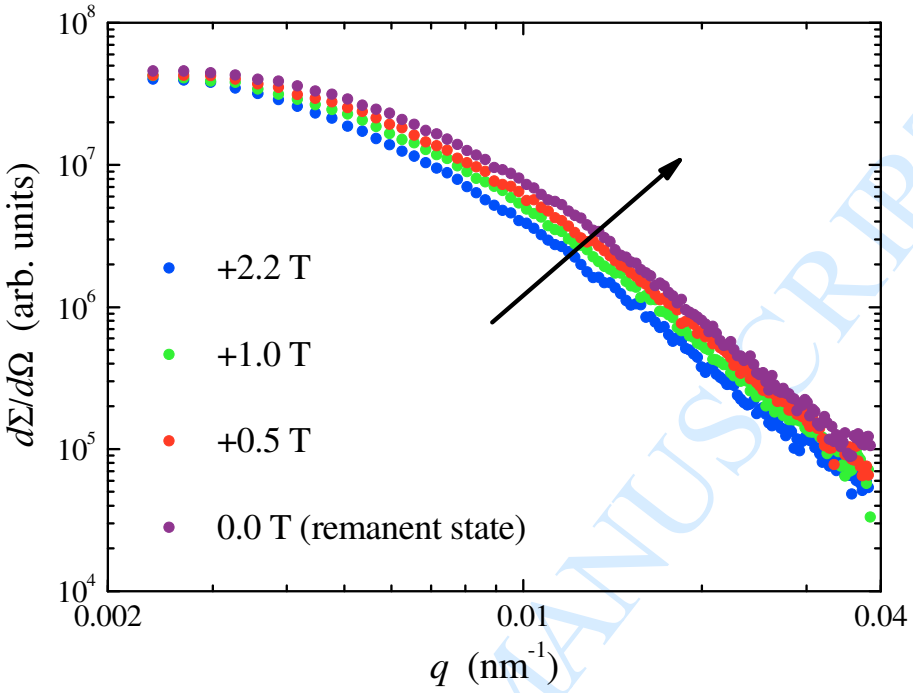

Figure 5(a)

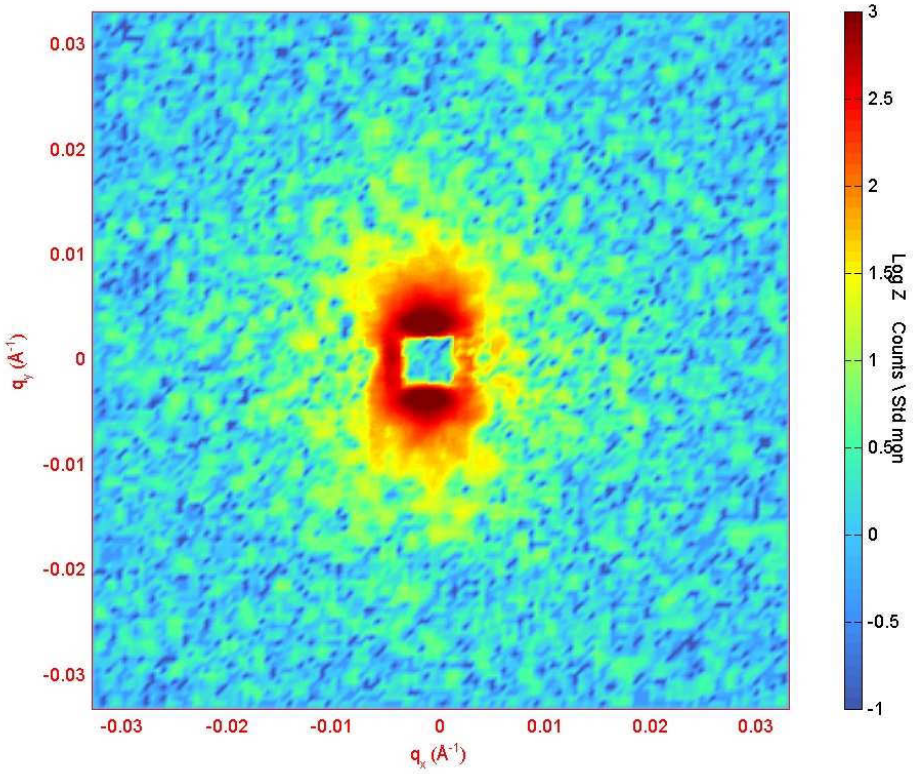

Figure 5(b)

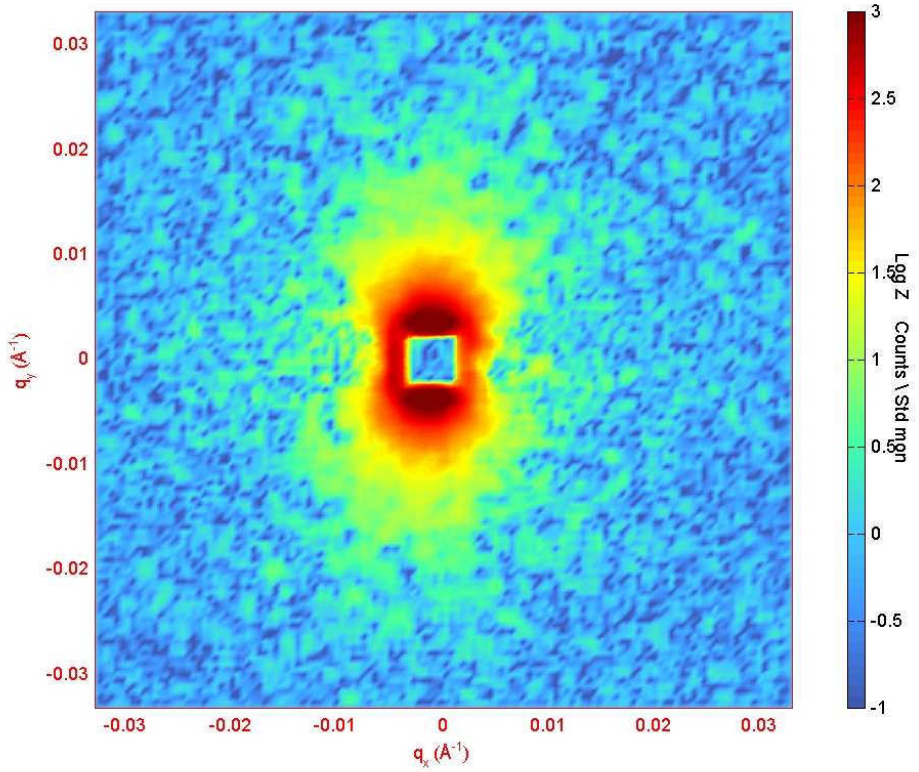

Figure 5(c)

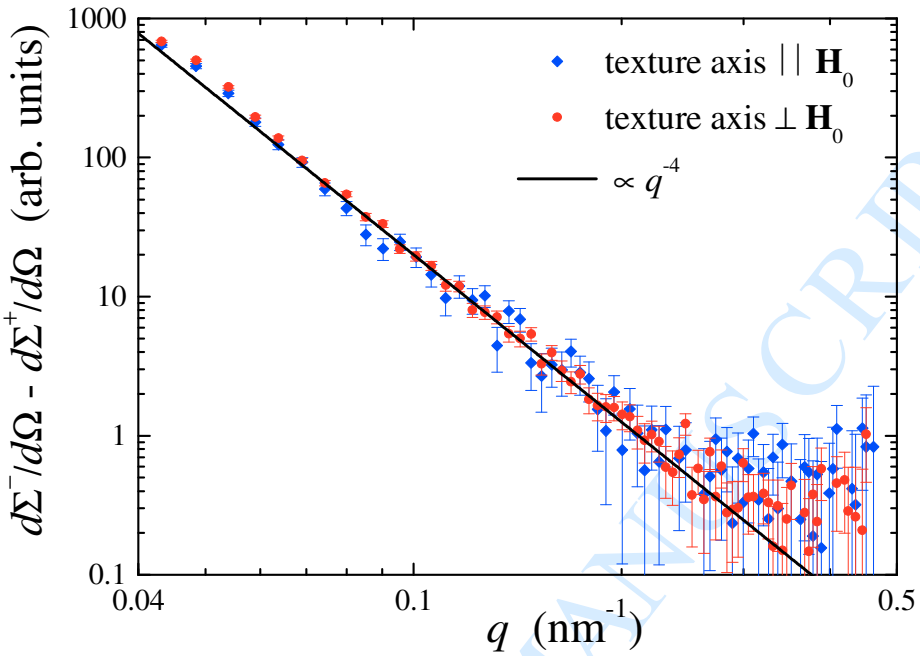

Magnetic microstructure of a textured Nd-Fe-B sintered magnet characterized by small-angle neutron scattering

E.A. Périgo[1], D. Mettus[1], E.P. Gilbert[2], P. Hautle[3], N. Niketic[3], B. van den Brandt[3], J. Kohlbrecher[3], P. McGuiness[4], Z. Fu,[5] and A. Michels[1]

[1] Physics and Materials Science Research Unit, University of Luxembourg, 162a avenue de la Faïencerie, L-1511 Luxembourg, Grand Duchy of Luxembourg

[2] Bragg Institute, ANSTO, Locked Bag 2001, Kirrawee DC, NSW 2232, Australia

[3] Paul Scherrer Institute, CH-5232 Villigen PSI, Switzerland

[4] Institute of Metals and Technology, Lepi pot 11, Sl-1000 Ljubljana, Slovenia

[5] Jülich Centre for Neutron Science (JCNS), Forschungszentrum Jülich GmbH, Outstation at MLZ, Lichtenbergstraße 1, D-85747 Garching, Germany

Highlights

The characterization of textured Nd-Fe-B magnets by small-angle neutron scattering is addressed.

Long-range spin-misalignment fluctuations exist up to the micron range.

Polarized neutrons provide evidence for the presence of coupled nuclear-magnetic nanometer-scale fluctuations.

SANS is a powerful technique for characterizing the magnetic microstructure of Nd-Fe-B magnets on a mesoscopic length scale (1 ~ 1000 nm).